Cement and Concrete Composites 88 (2018) 121–129

Contents lists available at ScienceDirect

Cement and Concrete Composites

journal homepage: www.elsevier.com/locate/cemconcomp

Corrosion products and corrosion-induced cracks of low-alloy steel and low-carbon steel in concrete

Jinjie Shi*, Jing Ming, Yamei Zhang, Jinyang Jiang

Jiangsu Key Laboratory of Construction Materials, School of Materials Science and Engineering, Southeast University, Nanjing, 211189, China

ARTICLE INFO

Article history:
Received 20 December 2016
Received in revised form
5 December 2017
Accepted 5 February 2018
Available online 6 February 2018

Keywords:
Low-alloy steel
Corrosion products
Cracks
Concrete
X-ray computed tomography

ABSTRACT

The distribution of corrosion products at the steel-concrete interface and the pattern of corrosion-induced cracks were characterized using X-ray computed tomography (X-CT) and environmental scanning electron microscopy (ESEM). A novel low-alloy reinforcing steel (LA steel) and the conventional low-carbon reinforcing steel (LC steel) embedded in concrete were subjected to impressed current accelerated corrosion. The results of Raman spectroscopy showed that non-protective lepidocrocite (γ-FeOOH) was the main corrosion products for LC steel, while stable and protective maghemite (γ-Fe_2O_3) and less crystallized feroxyhite (δ-FeOOH) and ferrihydrite ($5Fe_2O_3 \cdot 9H_2O$) were identified in the Cr-enriched inner rust layer of LA steel.

1. Introduction

Corrosion of steel reinforcements in concrete is one of the primary causes of structural deterioration of infrastructure in severe environments [1,2]. The steel reinforcements are initially protected by a protective passive film formed from alkaline concrete pore solutions. However, this passive film is unstable and finally depassivated when subjected to chlorides and atmospheric CO_2 [3]. After depassivation, corrosion products are formed at the steel-concrete interface. Since the volume of corrosion products is higher than the original steel, cracks initiate at the steel-concrete interface due to the increasing expansive pressure [4].

To mitigate the damage of concrete induced by steel corrosion, alloy steels with high performance-price ratio are becoming a growing concern as an alternative to low-carbon steel [5–16]. The most used alloying element in alloy steels is Cr, because its price is lower than Ni and Mo [13]. More importantly, both the passivation capability of steels and the corrosion resistance of the rust layer can be improved when an appropriate amount of Cr has been added in alloy steels [17].

Alloy steels with Cr content higher than 3 wt% were widely studied in previous researches [6,8,9,11,12,14–16]. It was reported that the passive film of Cr-bearing steels had better pitting corrosion resistance than low-carbon steels because $Cr(OH)_3$ can be formed in the passive film of Cr-bearing steels [8,15]. Due to the formation of more protective passive film, the chloride threshold level of Cr-bearing steels was much higher compared with low-carbon steel [11,12]. After depassivation, goethite (α-FeOOH) was the main iron oxide-hydroxides formed for Cr-bearing steel, which was considered as one of the protective corrosion products in chloride environments [6,9]. Although Cr-bearing steels with Cr content great than 3 wt% have much higher corrosion resistance than low-carbon steel, the poor weldability and high price, however, limit their large-scale popular use and field application [13,15].

Compared with low-carbon steel and high Cr-bearing steels, optimized low-alloy steel with trace alloying elements (<1 wt% Cr) provides several benefits, such as very low incremental cost, superior mechanical properties and good welding performance [13]. The high long-term corrosion resistance due to the formation of compact and protective rust layer is the most significant advantage of low-alloy steel [5,7,10]. Moreover, it should be noted that, the corrosion resistance of stainless steels and high-alloy steels is largely influenced by the presence of Cr depleted porous mill scale, which inhibit the formation of protective Cr-bearing passive film [16,18]. Therefore, the removal of mill scale from stainless steels is recommended by their manufacturers to improve their corrosion resistance, which will both increase the cost and pollute the

* Corresponding author.
E-mail address: jinjies@126.com (J. Shi).

https://doi.org/10.1016/j.cemconcomp.2018.02.002
0958-9465/

Table 1
Chemical compositions of LC and LA steels.

Element	LC (wt.%)	LA (wt.%)
C	0.22	0.20
Si	0.53	0.65
Mn	1.44	0.57
P	0.025	0.027
S	0.022	0.008
V	0.038	0.032
Cr	–	0.86
Cu	–	0.06
Ni	–	0.03
Fe	Bal.	Bal.

environment when stainless steels are used [13,18]. In low-alloy steels there is little Cr to be depleted in the mill scale and the presence of mill scale has less influence on their corrosion resistance [13]. Therefore, it is a desired alternative to conventional low-carbon steel for widespread use under field conditions.

However, most of the previous studies concerning the corrosion resistance of low-alloy steels were conducted in simulated concrete pore solutions [5,10]. Therefore, the effect of steel-concrete interface on the formation of passive film and corrosion products for low-alloy steels will be generally ignored [7,19,20]. Moreover, it is impossible to observe the formation and penetration of corrosion products and the evolution of corrosion-induced cracks in concrete cover, which are of great importance for the evaluation of the service life of reinforced concrete structures [21–25].

In order to get full understanding of the nature of the corrosion products of low-alloy steel with Cr content lower than 1 wt% as well as the distribution of corrosion-induced cracks in concrete, the active corrosion of low-carbon (LC) steel and low-alloy (LA) steel was induced by impressed current method in this study. The distribution of corrosion products and cracks was investigated by X-ray computed tomography (X-CT), optical microscopy (OM) and environmental scanning electron microscopy (ESEM) with energy dispersive X-ray spectroscopy (EDS). Raman spectroscopy was employed to identify the composition of corrosion products of LC and LA steels at the steel-concrete interface.

2. Experimental

2.1. Materials and specimens

The chemical compositions of LC steel and LA steel are shown in Table 1. Compared with LC steel, LA steel contains 0.86 wt% Cr and a small amount of alloying elements Cu and Ni. To improve the plasticity and weldability, the carbon content in LA steel is relatively lower than that in LC steel. The mechanical properties of LA steel are comparable to conventional LC steel, with tensile strength of 650 MPa, yield strength of 450 MPa and total elongation of 31% [26]. Fig. 1 shows the optical micrographs of the microstructure of LC and LA steels after etching. The optical micrographs of both LC and LA steels show two dominant phases, brighter ferrite phase and darker pearlite phase (a combination of ferrite and carbide), which is the typical microstructure for conventional low-carbon reinforcing steel [5].

Table 2
Chemical composition of Portland cement.

Oxide	wt.%
CaO	64.11
SiO_2	20.60
Al_2O_3	5.03
Fe_2O_3	4.38
MgO	1.46
SO_3	2.24
$Na_2O + K_2O$	0.57
Loss on ignition	1.30

Table 3
Mixture proportions of concrete specimens.

Material	kg/m^3
Cement	352
Water	187
Fine aggregate	705
Coarse aggregate	1057
w/c ratio	0.53

Portland cement (P·II 42.5R) was used for the preparation of concrete specimens. The chemical composition of Portland cement is given in Table 2. River sand with the fineness modulus of 2.40 and gravel with the maximum size of 10 mm were used as the fine aggregate and the coarse aggregate, respectively. The mixture proportions of concrete specimens are shown in Table 3.

A schematic sketch of the concrete specimen is shown in Fig. 2. A ribbed steel with the diameter of 10 mm was embedded centrally in concrete specimen with the cover depth of 20 mm. A copper wire was soldered to one end of the reinforcing steel for the accelerated corrosion. In order to obtain a constant exposure surface for the characterization of corrosion products, both ends of the steel were covered with epoxy resin coating, leaving a free exposure area of approximately 31.4 cm^2. The concrete specimens were demoulded after 24 h and then cured in the standard curing room (temperature = 20 ± 3 °C and RH > 90%) for 28 days. Three concrete specimens were prepared for each type of steel in this study.

2.2. Accelerated corrosion test

The accelerated corrosion set-up is shown in Fig. 3. The concrete

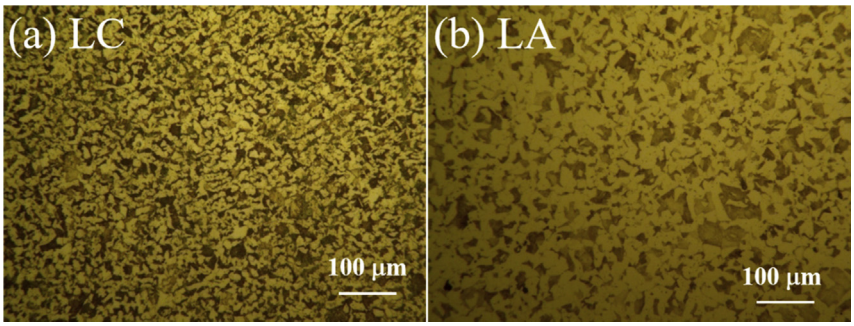

Fig. 1. Optical micrographs of etched steels.